SCALING OF TROPICAL-CYCLONE DISSIPATION

ÁLVARO CORRAL, ALBERT OSSÓ, AND JOSEP ENRIC LLEBOT

The influence of climate variability and global warming on the occurrence of tropical cyclones (TC) is a controversial issue Goldenberg *et al.* (2001); Trenberth (2005); Emanuel (2005a); Landsea (2005); Webster *et al.* (2005); Chan (2006); Klotzbach (2006); Shepherd & Knutson (2007); Kossin *et al.* (2007); Elsner *et al.* (2008). Existing historical databases on the subject are not fully reliable Kossin *et al.* (2007); Gray (2006); Landsea *et al.* (2006); Landsea (2007), but a more fundamental hindrance is the lack of basic understanding regarding the intrinsic nature of tropical cyclone genesis and evolution Emanuel (2005b). It is known that tropical cyclones involve more than a passive response to changing external forcing Emanuel (2008), but it is not clear which dynamic behaviour best describes them. Here we present a new approach based on the application of the power dissipation index (*PDI*), which constitutes an estimation of released energy Emanuel (2005a), to individual tropical cyclones. A robust law emerges for the statistics of *PDI*, valid in four different ocean basins and over long time periods. In addition to suggesting a novel description of the physics of tropical cyclones in terms of critical phenomena Bak (1996); Christensen & Moloney (2005), the law allows to quantify their response to changing climatic conditions, with an increase in the largest *PDI* values with sea surface temperature or the presence of El Niño phenomenon, depending on the basin under consideration. In this way, we demonstrate that the recent upswing in North Atlantic hurricane activity does not involve TCs quantitatively different from those in other sustained high-activity periods prior to 1970.

One important characterization of a complex phenomenon is given by the fluctuations in the "size" of the phenomenon over successive occurrences Bak (1996); Malamud (2004); Christensen & Moloney (2005). We refer to neither spatial size (area, volume) nor something like the Saffir-Simpson category Kantha (2006); rather, we seek a physically relevant measure of released energy. For a tropical cyclone, a reasonable proxy for this energy has been proposed by Emanuel Emanuel (2005a), using the *PDI*, defined as

$$PDI \equiv \sum_t v_t^3 \Delta t \ ,$$

where t denotes time and runs over the entire lifetime of the storm and v_t is the maximum sustained surface wind velocity at time t. In available best-track records, measurements are provided at intervals of $\Delta t = 6$ hours. Note that in this paper the *PDI* value is associated with an individual tropical cyclone, not with the total annual activity in some ocean basin Emanuel (2005a).

We analyze tropical cyclone best-track records for several ocean basins: the North Atlantic and Northeastern Pacific (from the National Hurricane Center Jarvinen *et al.* (1988)), and the Northwestern Pacific and the Southern Hemisphere (from the Joint Typhoon Warning Center Chu *et al.* (2002)). We exclude the North Indian Ocean, due to the small number of storms in the most reliable portion of its records. [For more details, see the Supplementary Information, Fig. S2.]

We display in Fig. 1(a) the *PDI* probability density, $D(PDI)$, normalized in the usual way ($\int_0^\infty D(PDI)dPDI = 1$), for all four basins. The distributions include all storms occurring during an extended period, either 1966-2007 or 1986-2007 as indicated in the legend. All four distributions (given vertical offsets for clarity) can be characterized by a power-law decay in their central regions,

$$D(PDI) \propto 1/PDI^{\alpha},$$

where the exponent α is in between 0.95 and 1.25 (Supplementary Information, including Table S1). Deviations from the power law at small *PDI* values can be attributed to the deliberate incompleteness of the records for "not significant" TCs, whereas the more rapid decay at large *PDI* values is associated with the finite size of the basin. That is, the storms with the largest *PDI* do not have enough room to last a longer time, as their tracks are limited by the size of the basin, which introduces a cutoff in the distribution (at its separation from the power-law fit, roughly) (Supplementary Information, Figs. S3-S7). Variations in the definition of the *PDI*, for example excluding times during which the storm attains subtropical or extratropical status, do not modify the shape of the *PDI* distribution; the results are also unchanged when restricted to storms that do not make continental landfall (Supplementary Information, Figs. S8 and S9).

The degree of similarity between the basins is truly remarkable, given the variety of formative processes at work. TCs in the Western Pacific (typhoons) develop principally from the monsoon, for example, while North Atlantic hurricanes are mainly associated with easterly waves (and the degree of association depends on the intensity of the hurricane) Shepherd & Knutson (2007); Landsea (1993). In addition, each regional centre or agency follows different protocols in obtaining their data, using techniques which have gradually improved Kossin *et al.* (2007); Gray (2006); Landsea *et al.* (2006); Landsea (2007).

Nevertheless, the shape of the *PDI* distribution is robust over long time periods. Figure 1(b) shows that this consistency holds over a period of at least 100 years in the North Atlantic (where the record is longest; corrections to the calibration of the maximum velocity do not alter this pattern, Supplementary Information, Fig. S10). Thus, even though the database is certainly incomplete prior to the satellite era, and even more unreliable before aircraft reconnaissance began in 1944, the fraction of missed storms seems to be independent of *PDI*. This finding may appear counterintuitive until we consider the fact that a long-lasting tropical cyclone might be recorded as two shorter storms if its track is lost at some point. A power-law distribution is robust against such splitting of the data (Supplementary Information).

The existence of a simple statistical distribution that describes the whole spectrum of tropical cyclone dissipation in different basins over a long period of time (apart from incompleteness and finite size effects) reflects a startling degree of unity in the phenomenon; the small tropical depressions are described in the same way as the full developed most severe storms. Moreover, a robust power-law distribution is the hallmark of scale invariance Christensen & Moloney (2005): there is no typical tropical cyclone *PDI*, up to the maximum allowed in a given ocean basin. The fact that all scales are equally important regarding the number of events poses a great challenge to the modelling of this complex phenomenon, and even to large-scale global climate simulations Emanuel (2008).

Scale invariance can occur in processes where perturbations propagate through a critical (i.e., highly susceptible) medium Bak (1996); Malamud (2004). Thus, our result could indicate that the atmosphere, or perhaps the ocean-atmosphere system, is close to a critical state. In fact, this idea is not new; already in the 70's it was suggested that atmospheric convection takes place in a near-unstable environment Arakawa & Schubert (1974). Much more recently, Peters and Neelin have demonstrated the existence of a non-equilibrium stability-instability transition to which the state of the atmosphere is attracted Peters & Neelin (2006). Some properties of this transition can be obtained from static images of convecting cloud fields Peters *et al.* (2009) or local observations of precipitation Peters *et al.* (2002). These findings support our complex-system approach to tropical-cyclone evolution; in correspondence, we provide a complementary perspective to the puzzle that these atmospheric processes constitute. It would be interesting to study if other nearly universal statistical properties of tropical cyclones can accommodate into this framework Emanuel (2000).

In addition, an important property of critical systems is that perturbations can evolve while keeping a delicate balance between growth and attenuation, resulting sometimes in sudden intensifications and deintensifications. Although recent years have seen considerable improvement in the prediction of tropical cyclone trajectories, reliable forecasts of their intensities have not yet been achieved Willoughby (2007); ver (2008). This failure may not be just due to technical limitations; it may be a fundamental feature of the criticality of tropical cyclone evolution.

In fact, we can draw a strong parallelism between tropical cyclones and earthquakes, as the law reported here is analogous to the well-known Gutenberg-Richter (GR) law of seismic occurrence. This law states that, for a given region, the distribution of earthquake magnitudes M is an exponential function, $D(M) \propto 10^{-bM}$, with $b \simeq 1$; however, in terms of seismic moment, and also in terms of radiated energy E, the GR law turns out to be a power law, $D(E) \propto 1/E^{1+2b/3}$ (as energy is supposed to be proportional to seismic moment, which is an exponential function of magnitude, i.e., $E \propto 10^{3M/2}$). Nevertheless, the finite-size effects present in tropical cyclones are not so clear in earthquakes Main *et al.* (2008).

Tropical cyclone activity shows large interannual variability. One important factor controlling such variability is sea surface temperature (*SST*). We average *SST* from the

Hadley Center Rayner *et al.* (2003) over the same spatial areas and months in the TC season than Webster *et al.* Webster *et al.* (2005) in order to get an annual (so, seasonal) SST value for each basin; then, we separate the PDI density into two contributions, one for years with SST above its long-term mean value $\langle SST \rangle$ (i.e., high SST) and another one for SST below $\langle SST \rangle$ (low SST). Mathematically, $\langle SST \rangle \equiv \sum_y SST(y)/Y$, where $SST(y)$ refers to year y and Y is the total number of years. In this way we eliminate the effect of interannual variations in the number of TCs and concentrate on a comparison of the individual tropical cyclones characterizing each type of year.

Remarkably, for the North Atlantic and the Northeastern Pacific, the resulting distributions have essentially the same shape as the distribution for all years but with a difference in scale: high-SST years are characterized by a larger value of the finite-size cutoff, and conversely for low-SST years, as can be seen in Fig. 2(a). The other two basins show much minor PDI variation with SST.

If we rescale each conditional distribution by a power of its mean value, $\langle PDI \rangle$, such that $PDI \to PDI/\langle PDI \rangle^{\nu}$ and $D(PDI) \to \langle PDI \rangle^{\beta} D(PDI)$, with $\nu = \beta = 1$ if $\alpha \leq 1$, and $\nu = 1/(2-\alpha)$ and $\beta = \alpha/(2-\alpha)$ if $\alpha > 1$, it becomes apparent that, for each basin, both distributions share a similar shape, as shown in Fig. 2(b). (The reason of this rescaling is the fact that a distribution with $\alpha > 1$ does not scale linearly with its mean value, see Supplementary Information.) Then, the difference between high-SST and low-SST PDI distributions rests mainly in the scale of the finite-size cutoff and not in the shape of the distribution. A more detailed analysis shows also small changes in the value of the exponents (Supplementary Information).

Years with high SST are thus characterized by hurricanes with larger PDI values. As the PDI integrates the cube of the velocity over the storm lifetime, larger PDI values can result from longer lifetimes, larger (6-hour) velocities, or both. An analysis of the distributions of these variables shows that the increase in PDI comes mainly from an increase in the velocities, most apparent in the range above about 100 knots (i.e., corresponding to category 3 hurricanes and beyond Webster *et al.* (2005)), in comparison with years of low SST (Supplementary Information, Fig. S11).

An analogous study can be done as a function of the so-called MEI index Wolter & Timlin (1998), which quantifies the strength of El Niño phenomenon. Taking annual values of MEI, years with $MEI > 0$ (corresponding to El Niño) lead to increased PDI values in the Northeastern and Northwestern Pacific, but keeping again a similar shape of the PDI distribution, and the opposite when $MEI < 0$, see Figs. 2(a) and 2(b). In the case of the Northwestern Pacific, the contribution of TC lifetimes to the increase in PDI is larger than in the rest of the cases (Supplementary Information). This is somehow related to the findings of Refs. Lander (1994); Emanuel (2007). Very little variation with MEI is observed in the other two basins. Other indices (AMO, NAO, etc.) do not seem to influence the PDI distribution in any basin.

It is a well-known fact that individual years of high (or low) TC activity cluster into longer periods of predominantly high (or low) activity. For example, the North Atlantic has seen extraordinarily high activity between 1995 and 2005, which has been linked to global warming through an increase in the sea surface temperature Emanuel (2005a); Webster *et al.* (2005) (the issue is nonetheless controversial Landsea (2005); Chan (2006); Gray (2006)). According to our analysis, the *PDI* distribution for the period 1995-2005 is clearly different from the one for 1971-1994 (in agreement with Ref. Emanuel (2005a)), but it is indistinguishable from the distribution for years with high *SST* between 1966 and 2007, as well as from the distribution for other periods of high activity, like 1945-1970 Goldenberg *et al.* (2001), see Fig. **??**. With the necessary reservations when analyzing old hurricane records, we conclude that, so far, the recent dramatic increase of North Atlantic activity has not led to unprecedented energy releases by individual hurricanes.

Methods

The figures show estimations of the *PDI* probability density, $D(PDI)$. For any variable quantity X, its probability density is defined as $D_X(x) \equiv \text{Prob}[x \leq \text{ variable } < x+dx]\,/\,dx$, with $dx \to 0$ in the ideal case (we omit the label X although for instance for earthquakes $D(M)$ and $D(E)$ are different functions indeed). In practice, $D(x)$ is estimated as the number of cases $n(x)$ between x and $x+\Delta x$ divided by the total number of cases and by Δx. For power laws and other long-tailed distributions it is recommended not to take a constant Δx but a Δx that is proportional to x (in our case, $(x+\Delta x)/x \simeq 1.6$), which is referred to as logarithmic binning, due to the fact that in a log-log scale the bins appear as having constant size. Error bars for $D(x)$ can be estimated as $\varepsilon(x) \simeq D(x)/\sqrt{n(x)}$ corresponding to one-standard-deviation uncertainty (see Supplementary Methods).

Nevertheless, the plots of $D(PDI)$ are only illustrative as our estimations of the power-law exponent α are independent on the estimation of $D(PDI)$. Instead of fitting a straight line to the log-log plots of $D(PDI)$, we use maximum likelihood estimation. The goodness of the fit is addressed with the Kolmogorov-Smirnov test (which uses the estimation of the cumulative distribution function) and the corresponding $p-$value is obtained from Monte Carlo simulations, as explained in detail in the Supplementary Information.

References

Goldenberg, S. B., Landsea, C. W., Mestas-Nuñez, A. M. & Gray, W. M. The Recent Increase in Atlantic Hurricane Activity: Causes and Implications. *Science* **293**, 474–479 (2001).

Trenberth, K. Uncertainty in Hurricanes and Global Warming. *Science* **308**, 1753–1754 (2005).

Emanuel, K. Increasing destructiveness of tropical cyclones over the past 30 years. *Nature* **436**, 686–688 (2005a).

Landsea, C. W. Hurricanes and global warming. *Nature* **438**, E11–E12 (2005).

Webster, P. J., Holland, G. J., Curry, J. A. & Chang, H.-R. Changes in Tropical Cyclone Number, Duration, and Intensity in a Warming Environment. *Science* **309**, 1844–1846 (2005).

Chan, J. C. L. Comment on "Changes in Tropical Cyclone Number, Duration, and Intensity in a Warming Environment". *Science* **311**, 1713b (2006).

Klotzbach, P. J. Trends in global tropical cyclone activity over the past twenty years (1986-2005). *Geophys. Res. Lett.* **33**, L10805 (2006).

Shepherd, J. M. & Knutson, T. The Current Debate on the Linkage Between Global Warming and Hurricanes. *Geography Compass* **1**, 1–24 (2007).

Kossin, J. P., Knapp, K. R., Vimont, D. J., Murnane, R. J. & Harper, B. A. A globally consistent reanalysis of hurricane variability and trends. *Geophys. Res. Lett.* **34**, L04815 (2007).

Elsner, J. B., Kossin, J. P. & Jagger, T. H. The increasing intensity of the strongest tropical cyclones. *Nature* **455**, 92–95 (2008).

Gray, W. M. Comments on "Increasing destructiveness of tropical cyclones over the past 30 years". *http://arxiv.org* **0601050** (2006).

Landsea, C. W., Harper, B. A., Hoarau, K. & Knaff, J. A. Can We Detect Trends in Extreme Tropical Cyclones? *Science* **313**, 452–454 (2006).

Landsea, C. W. Counting Atlantic Tropical Cyclones Back to 1900. *Eos* **88 (18)**, 197–202 (2007).

Emanuel, K. *Divine Wind: the History and Science of Hurricanes* (Oxford University Press, New York, 2005b).

Emanuel, K. The Hurricane-Climate Connection. *Bull. Am. Met. Soc.* **(5)**, ES10–ES20 (2008).

Bak, P. *How Nature Works: The Science of Self-Organized Criticality* (Copernicus, New York, 1996).

Christensen, K. & Moloney, N. R. *Complexity and Criticality* (Imperial College Press, London, 2005).

Malamud, B. D. Tails of natural hazards. *Phys. World* **17 (8)**, 31–35 (2004).

Kantha, L. Time to Replace the Saffir-Simpson Hurricane Scale? *Eos* **87 (1)**, 3–6 (2006).

Jarvinen, B. R., Neumann, C. J. & David, M. A. S. A tropical cyclone data tape for the North Atlantic basin, 1886-1983: contents, limitations, and uses. *http://www.nhc.noaa.gov/pdf/NWS-NHC-1988-22.pdf* (1988).

Chu, J.-H., Sampson, C. R., Levine, A. S. & Fukada, E. The Joint Typhoon Warning Center Tropical Cyclone Best-Tracks, 1945-2000. *https://metocph.nmci.navy.mil/jtwc/best_tracks/TC_bt_report.html* (2002).

Landsea, C. W. A climatology of intense (or major) hurricanes. *Mon. Weather Rev.* **121**, 1703–1713 (1993).

Arakawa, A. & Schubert, W. H. Interaction of a cumulus cloud ensemble with the large-scale environment, part I. *J. Atmos. Sci.* **31**, 674–701 (1974).

Peters, O. & Neelin, J. D. Critical phenomena in atmospheric precipitation. *Nature Phys.* **2**, 393–396 (2006).

Peters, O., Neelin, J. D. & Nesbitt, S. W. Mesoscale convective systems and critical clusters. *J. Atmos. Sci.* 2913–2924 (2009).

Peters, O., Hertlein, C. & Christensen, K. A Complexity View of Rainfall. *Phys. Rev. Lett.* **88**, 018701 (2002).

Emanuel, K. A Statistical Analysis of Tropical Cyclone Intensity. *Mon. Wea. Rev.* **128**, 1139–1152 (2000).

Willoughby, H. E. Forecasting Hurricane Intensity and Impacts. *Science* **315**, 1232–1233 (2007).

National Hurricane Center Forecast Verification. *http://www.nhc.noaa.gov/verification* (2008).

Main, I. G., Li, L., McCloskey, J. & Naylor, M. Effect of the Sumatran mega-earthquake on the global magnitude cut-off and event rate. *Nature Geosci.* **1**, 142 (2008).

Rayner, N. A. *et al.* Global analyses of sea surface temperature, sea ice, and night marine air temperature since the late nineteenth century. *J. Geophys. Res.* **108 (D14)**, 4407 (2003).

Wolter, K. & Timlin, M. S. Measuring the strength of ENSO events: how does 1997/98 rank? *Weather* **53(9)**, 315–324 (1998).

Lander, M. A. An Exploratory Analysis of the relationship between Tropical Storm Formation in the Western North Pacific and ENSO. *Mon. Weather Rev.* **122**, 636–651 (1994).

Emanuel, K. Environmental Factors Affecting Tropical Cyclone Power Dissipation. *J. Clim.* **20**, 5497–5509 (2007).

Supplementary Information

Available.

Acknowledgements

We have benefited from the expertise and kindness of A. Clauset, A. Deluca, K. Emanuel, E. Fukada, A. González, J. Kossin, B. Mathiesen, M. Paczuski, O. Peters, G. B. Raga, R. Romero, and A. Turiel. A.O. and A.C. were put in contact through G. Orriols. The initial part of our research has been financed by the EXPLORA - INGENIO 2010 program, grant FIS2007-29088-E, and also partially by FIS2009-09508, CGL2007-60797/CLI, and 2009SGR-164. A.C. is also a participant of the CONSOLIDER i-MATH project.

Author Contributions

A.O. downloaded the data, A.C. wrote most of the codes, A.O. and A.C. analyzed the data, A.C. wrote the paper, J.E.L. provided feedback, support and participated in discussions, A.C. struggled with the reviewers.

Author Information

Correspondence and requests for materials should be addressed to A.C. (ACorral at crm dot cat).

Competing financial interests

The authors declare no competing financial interests.

FIGURE 1. | **Power-law distributions of tropical-cyclone *PDI* values.** (a) *PDI* probability densities for tropical cyclones in the North Atlantic, Northeastern Pacific, Northwestern Pacific, and Southern Hemisphere basins. The period considered is either 1966-2007 or 1986-2007, as indicated in the legend, depending on the reliability of the records and the sufficiency of statistics. The values in the vertical axis are divided by the factors 1, $\sqrt{1000}$, 1000 and $\sqrt{1000^3}$, to separate the curves for clarity. The distributions are consistent with a power law (straight lines) over some portion of their range, with exponents $\alpha = 1.19 \pm 0.06$, 1.175 ± 0.05, 0.96 ± 0.02 and 1.11 ± 0.04, from top to bottom and the Kolmogorov-Smirnov (KS) test yields $p-$values larger than 20 % in all basins (Supplementary Information). Deviations from the power law at large *PDI* values reflect the finite size effect. (b) *PDI* probability densities for tropical cyclones in the North Atlantic over the 54-year periods 1900-1953 and 1954-2007, with 436 and 579 storms and $\alpha = 1.09 \pm 0.04$ and 1.17 ± 0.04 (straight lines), respectively. A two-sample KS test (Supplementary Information) gives a $p-$value around 15% (51% if $PDI > 2 \cdot 10^9 \, m^3/s^2$). The robustness of the distribution is apparent despite a notable lack of homogeneity in the quality of records.

FIGURE 2. | **Scaling of *PDI* distributions conditioned to *SST* and El Niño.** (a) *PDI* probability densities calculated separately for years with high or low *SST* and for years with $MEI > 0$ or $MEI < 0$. Tropical depressions (storms whose maximum v_t is below 34 knots, 1 knot = 1.85 km/h) are excluded from the Northwestern Pacific dataset, in order to give all basins the same treatment. Time periods and vertical offsets are as in Fig. 1(a). In all cases the data can be fit by a power law, being the worst one that of the North Atlantic with low *SST*, which yields $\alpha = 1.26 \pm 0.08$ with $p = 9\%$. (b) As with the previous panel, except that the unconditioned distributions and their fits are included, and the axes are rescaled by $\langle PDI \rangle^{\nu(\alpha)}$ and $1/\langle PDI \rangle^{\beta(\alpha)}$ with $\alpha = 1.19$, 1.175, 1.175 and 1.0 (the data sets at the bottom have been shifted extra factors 100 and 10^4 in each axis for clarity sake); the ratios of mean *PDI* between high and low annual values of *SST* or *MEI*, $\langle PDI \rangle_{high}/\langle PDI \rangle_{low}$, are 1.4, 1.6, 1.4, and 1.4, always from top to bottom.

FIGURE 3. | **Equivalence between periods of predominantly high activity and high *SST* in the North Atlantic.** Comparison of *PDI* probability densities for the years 1995-2005 and 1945-1970, as well as for years with high *SST* during 1966-2007. The number of storms is 166, 257 and 250, and the power-law exponent $\alpha = 1.00 \pm 0.06$, 1.02 ± 0.07 and 1.13 ± 0.08, respectively. A single fit to the 3 data sets yields $\alpha = 1.05 \pm 0.05$ with $p = 92\%$ (straight line). Two-sample KS tests yield $p-$values larger than 35% for each pair of distributions (Supplementary Information, Table S2); so we can conclude that no significant difference in the energy of TCs can be observed between these periods.

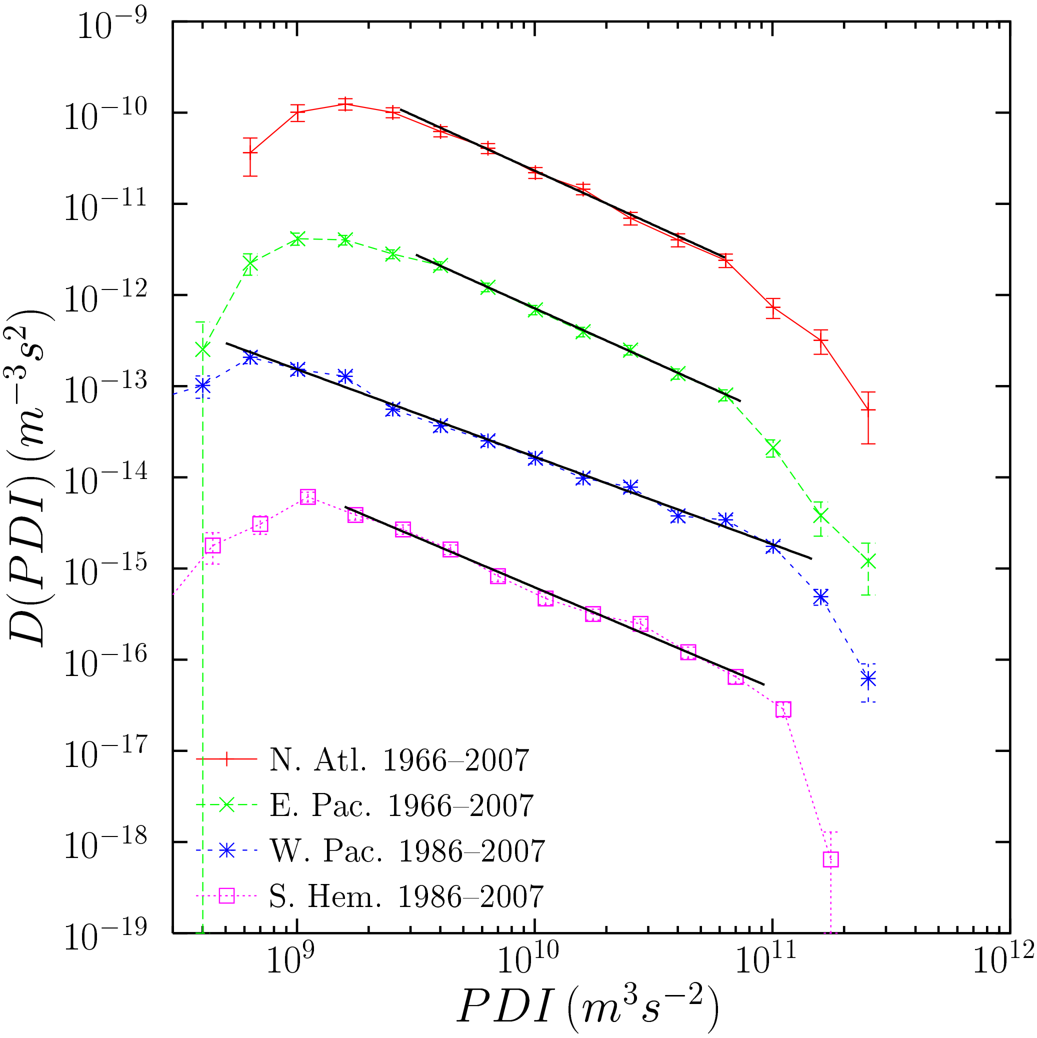
10^{-9}
10^{-10}
10^{-11}
10^{-12}
10^{-13}
10^{-14}
10^{-15}
10^{-16}
10^{-17}
10^{-18}
10^{-19}
$D(PDI)\,(m^{-3}s^2)$
N. Atl. 1966–2007
E. Pac. 1966–2007
W. Pac. 1986–2007
S. Hem. 1986–2007
10^{9}
10^{10}
10^{11}
10^{12}
$PDI\,(m^3s^{-2})$

1(a)

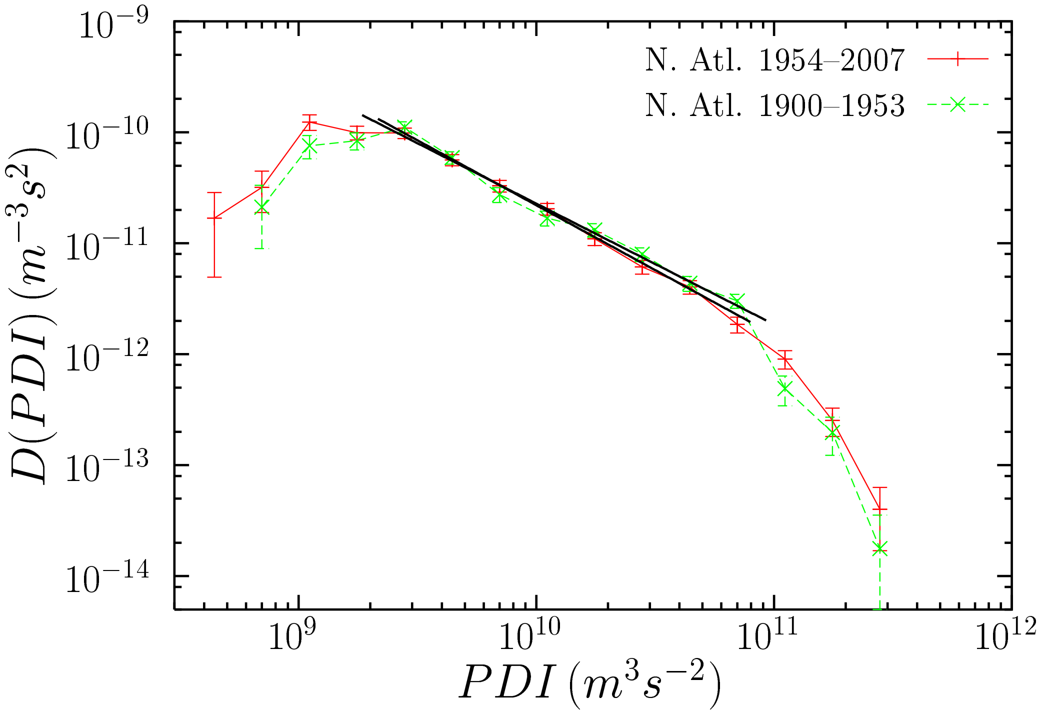
N. Atl. 1954–2007
N. Atl. 1900–1953
$D(PDI)\,(m^{-3}s^{2})$
$PDI\,(m^{3}s^{-2})$
10^{-9}
10^{-10}
10^{-11}
10^{-12}
10^{-13}
10^{-14}
10^{9}
10^{10}
10^{11}
10^{12}

1(b)

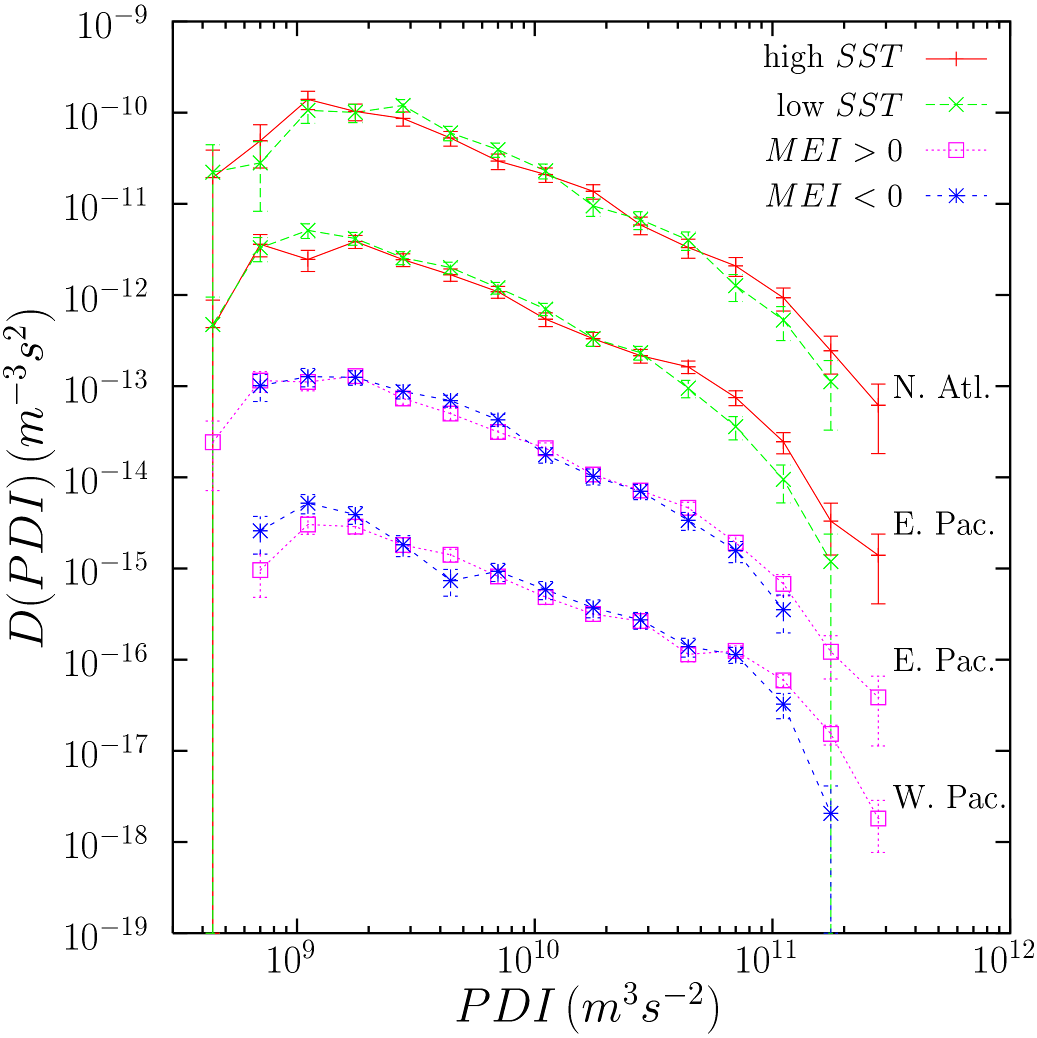
high SST
low SST
$MEI > 0$
$MEI < 0$
N. Atl.
E. Pac.
E. Pac.
W. Pac.
$D(PDI)\,(m^{-3}s^2)$
$PDI\,(m^3s^{-2})$
10^{-9}
10^{-10}
10^{-11}
10^{-12}
10^{-13}
10^{-14}
10^{-15}
10^{-16}
10^{-17}
10^{-18}
10^{-19}
10^{9}
10^{10}
10^{11}
10^{12}

2(a)

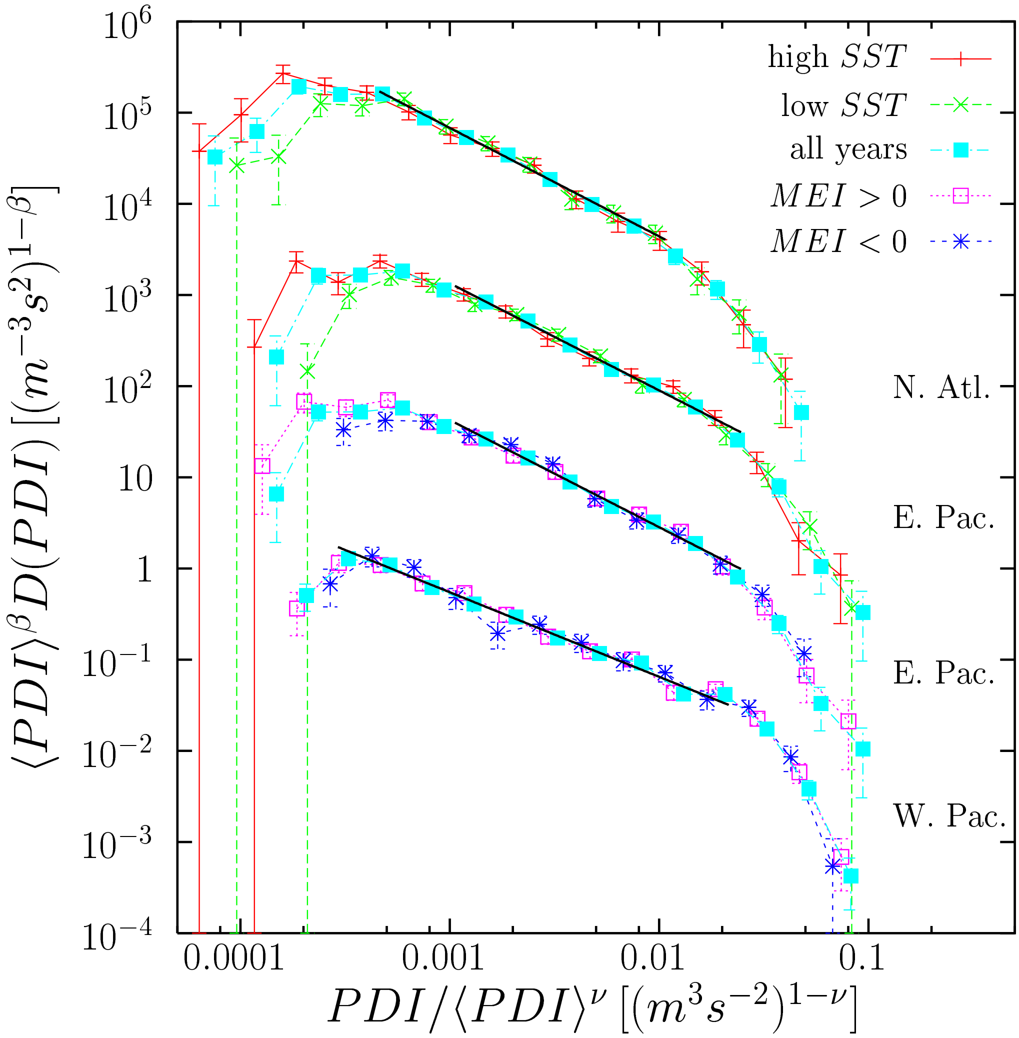

high SST
low SST
all years
$MEI > 0$
$MEI < 0$
N. Atl.
E. Pac.
E. Pac.
W. Pac.
10^6
10^5
10^4
10^3
10^2
10
1
10^{-1}
10^{-2}
10^{-3}
10^{-4}
0.0001
0.001
0.01
0.1
$\langle PDI\rangle^\beta D(PDI)\,[(m^{-3}s^2)^{1-\beta}]$
$PDI/\langle PDI\rangle^\nu\,[(m^3s^{-2})^{1-\nu}]$

2(b)

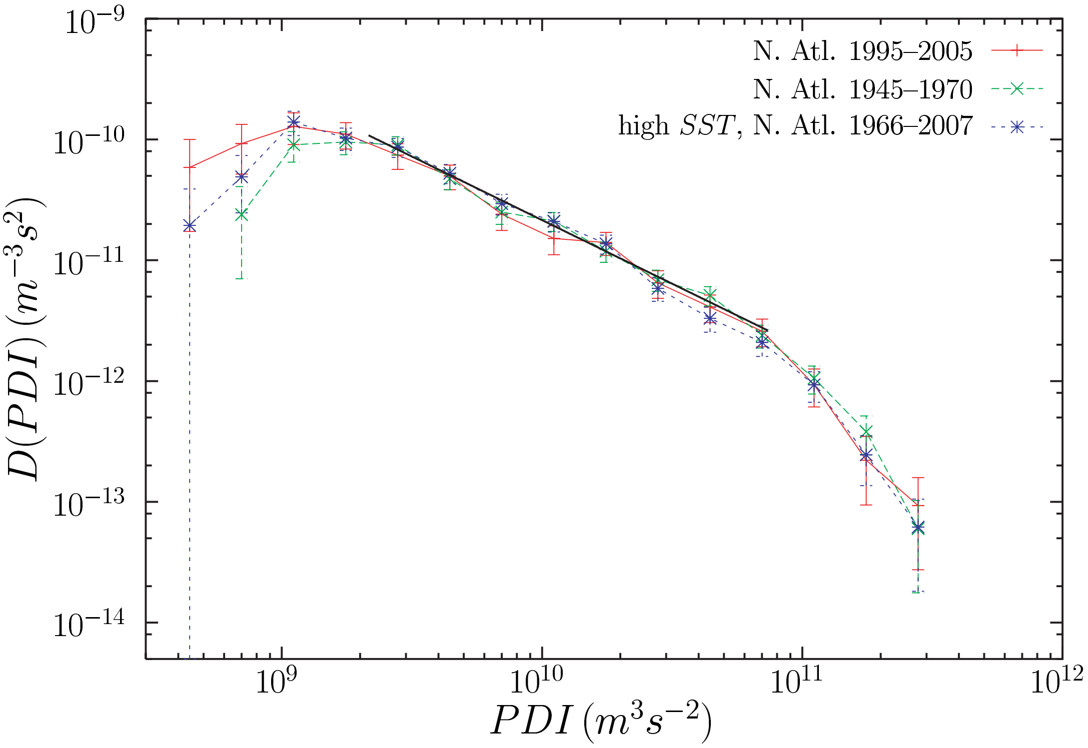
N. Atl. 1995–2005
N. Atl. 1945–1970
high SST, N. Atl. 1966–2007
$D(PDI)\,(m^{-3}s^{2})$
$PDI\,(m^{3}s^{-2})$
10^{-9}
10^{-10}
10^{-11}
10^{-12}
10^{-13}
10^{-14}
10^{9}
10^{10}
10^{11}
10^{12}

3

Álvaro Corral
Centre de Recerca Matemàtica
Edifici Cc, Campus Universitari
E-08193 Bellaterra, Barcelona
Spain

Albert Ossó & Josep Enric Llebot
Grup de Física Estadística
Facultat de Ciències
Universitat Autònoma de Barcelona
E-08193 Bellaterra, Barcelona
Spain